Paper No 2

Tire Innerliner Analysis for NHTSA Tire Aging Test Development Project

By Edward R Terrill*, Ana C. Barbur, and Mario J. Maffei
Akron Rubber Development Laboratory, Inc.
2887 Gilchrist Rd.
Akron, Ohio 44305

Presented at a meeting of the
Rubber Division American Chemical Society
Louisville, KY
October 14-16, 2008

* Speaker

Note from the National Highway Traffic Safety Administration
"This research was supported (in part) by the National Highway Traffic Safety Administration (NHTSA), U.S. Department of Transportation, under Contract DTNH22-03-D-18660. The opinions, findings and recommendations contained herein are those of the authors, and do not necessarily represent those of the NHTSA."

Abstract
A project to develop an accelerated aged endurance test for tires is being conducted by the United States Department of Transportation - National Highway Traffic Safety Administration. Six models of tires were collected from service in Phoenix Arizona, USA and a wide assortment of material tests were conducted on various rubber compounds in the tires to track the evolution of properties during on-vehicle service. Scientific literature attributes the evolution of changes in properties of the rubber compounds and their interfaces to thermal-oxidation. A key tire component affecting thermal-oxidation in tires is the tire innerliner because it slows the diffusion of oxygen from the tire cavity to tire compounds. An understanding of the tire innerliners was desired including innerliner composition. The innerliner composition of the six NHTSA tire brands from the NHTSA tire data set (NHTSA tire types B, C, D, E, H, and L) were analyzed for composition. In addition, the compositions of innerliners from another 37 tire types were analyzed. The analytical techniques used to determine the liner compositions included X-ray fluorescence spectroscopy, energy dispersive X-ray spectroscopy, pyrolysis-gas chromatography /flame ionization detector, and pyrolysis-gas chromatography /mass spectroscopy. The innerliner composition correlated with liner permeability. Innerliner permeability was measure on extracted liner slices. The permeability results were correlated with the compositional results, for which butyl content was a major factor affecting permeability rates.

Purpose and Scope:
This report emphasizes the innerliner characteristics observed in a wide range of tire types and brands. The characterization included chemical composition and permeability from thin slices extracted from tires. The techniques for determining the composition and permeability of innerliner compounds extracted from tires are described herein. Many analytical characterization methods were developed in the course of this project, including the extraction of thin slices of innerliner from tires. The liner permeability data was correlated with liner composition.

Background
Tires of various models used in this paper were collected from on-vehicle service in Phoenix Arizona, USA and analyzed by NHTSA during development of an accelerated tire durability test.[1] Scientific literature attributes the changes in properties of the rubber compounds and their interfaces to thermal-oxidation.[29-31] One key tire component affecting thermal-oxidation in tires is the tire innerliner, because of its ability to slow diffusion of oxygen from the tire cavity to tire components during service. Several authors have described the effect of liner composition on liner permeability.[5-7] They showed the effects of liner permeability and liner gauge on intra-carcass pressure and inflation pressure retention. The effect of compound variables on innerliner permeability

has been studied.[8, 9] D. M. Coddington showed the correlation between innerliner permeability, oxidation, and belt edge durability during road wheel testing.[6]

Experimental

Tire Dissection: The tires were dissected to remove the innerliner compound for testing.

Pyrolysis-gas chromatography/flame ionization detector (GC/FID): This method provided quantification of butyl rubber, natural rubber, polybutadiene rubber, and styrene butadiene rubber in rubber compounds.[18-19] The analytical system consisted of a PerkinElmer Clarus 500 GC/FID interfaced with a CDS Analytical Pyroprobe 5000 Pyrolysis Autosampler. Samples were loaded into the pyroprobe (Figure 1). Samples were rapidly pyrolyzed at 550°C. The volatiles and degradation products were automatically introduced into the GC carrier stream and transferred to the GC column equipped with a non-polar capillary column for analysis by GC/FID (Figure 2). Only monomer peaks (isobutylene, isoprene, styrene, and butadiene) having the highest intensity were used for the calibration. A piece of sample about 0.5 mg was used. To have sufficient separation between isobutylene and 1,3 butadiene, the GC oven was cooled down to -20C, using liquid nitrogen. The tests duration was about 40 minutes. The detection limits are about +/-5 weight percent for the polymer components in the formulation. The peak assignments and calibration are in the discussion section.

Figure 1: Loading Sample into Pyroprobe

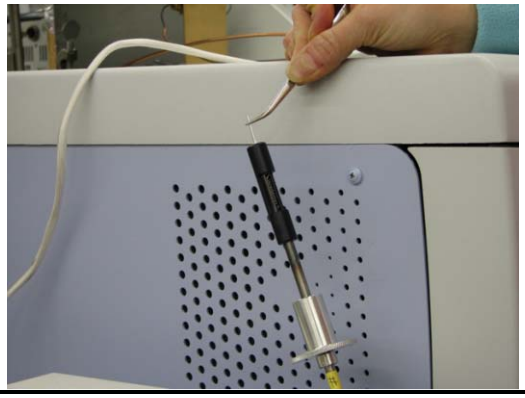

Figure 2: Running Sample in Pyrolysis-GC/MSFID

Pyrolysis-gas chromatography/mass spectroscopy (GC/MS): This method has been used to quantify butyl rubber, natural rubber, polybutadiene rubber, and styrene butadiene rubber in rubber compounds.[12-20] The analytical system consisted of a PerkinElmer Clarus 500 GC/ 560D MS interfaced with a CDS Analytical Pyroprobe 5000 Pyrolysis Autosampler. Samples were rapidly pyrolyzed at 550°C. The volatiles and degradation products were automatically introduced into the GC carrier stream and transferred to the GC column equipped with a non-polar capillary column for analysis by GC/MS. A piece of sample about 0.2 mg was used. The tests duration was about 40 minutes. The detection limits are about +/-5 weight percent for the polymer components in the formulation. The peak assignments and calibration are in the discussion section.

Energy Dispersive X-ray Fluorescence (XRF): The method used a Jordan Valley EX-3600M TEC Laboratory Spectrometer for qualitative determination of solid samples for element of atomic mass greater than sodium (Figure 3).[21-22] The results are reported in three different concentration groups, ie major (>1%), minor (100ppm-1%, traces (<100ppm). The sample was placed into a disposable cup. The X-ray source was a palladium tube using a 45kV accelerating voltage. One set of spectra was the result of analysis with a titanium target. In the titanium secondary target analysis the source was pointed at the target and the target element was excited and fluoresced. Then the target fluorescence was used to excite the sample. The titanium target increased the sensitivity for the light elements (Figure 4). This was utilized for the analysis and detection of the following elements (Sulfur, Silicon, Potassium, and Calcium). The second sets of spectra were analyzed with a Collimator. A collimator was placed between the source and sample to reduce signal (background). This technique was used for the remaining elements (Bromine, Iron, Zinc, and Chlorine) (Figure 5). The elements contained in the sample are thereby excited to emit the element specific X-ray fluorescence radiation. A liquid nitrogen cooled light element detector (LED) Si(Li) measured the fluorescent and scattered x-rays from the sample as a multichannel analyzer and software assigned each pulse an energy value thus produced the spectrum.

Figure 3: ED-XRF Equipment

Figure 4: ED-XRF Output for Light Elements

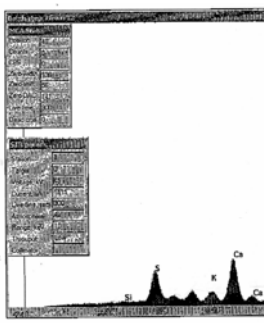

Figure 5: ED-XRF Output for Heavy Elements

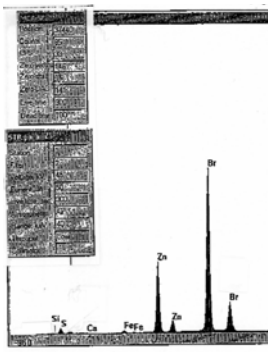

Energy Dispersive X-ray Spectroscopy (EDAX): The sample was prepared by placing the tire innerliner on an aluminum pin mount coated with double-sided carbon adhesive tape. EDAX was used in conjunction with the scanning electron microscope providing chemical analysis (Figure 6). EDAX can detect all elements except H, He, Li, and Be. Tire innerliners were analyzed using a Cambridge S150T SEM interfaced with an EDAX PV9800 X-ray detector and IXRF EDS2004 X-ray analysis computer software. The Backscatter Detection (BSD) mode was used for imaging. Energy Dispersive X-ray (EDX) analysis was done on elements above Sodium (Na) in the periodic table in the energy range from 0 KeV to 20 KeV (Figure 7). The x-ray spectral lines were calibrated using a copper/aluminum standard to assure correct identification of the elements. Automatic baseline correction is used and only those elements above the background matrix are reported. Results should be considered as being semi-quantitative. It should be kept in mind that only an area approximately 1.1 mm^2 was being analyzed, and the sample may not be homogenous over a larger area. The beam energy used was 20 KeV, which would penetrate the surface to a depth of about 7μm. The results reflect the relative amounts of the elements present in the surfaces of the samples to this depth. All samples were analyzed in the same manner using ZAF correction for the semi-quantitative analysis at a sample tilt of 20°. Figure 5 is an EDX spectrum of a sample. All data for each sample was normalized to 100%.

Figure 6: SEM/EDAX Equipment

Figure 7: EDAX Output

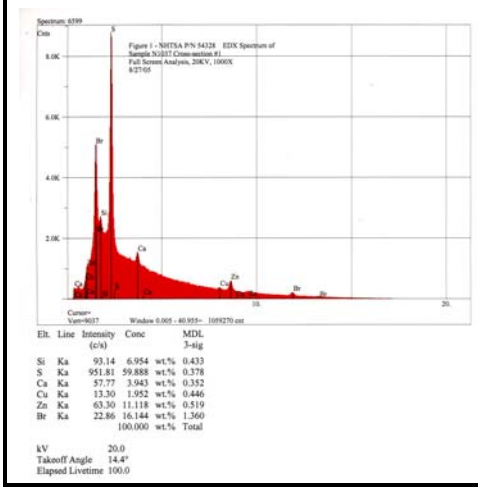

Elt.	Line	Intensity (c/s)	Conc		MDL 3-sig
Si	Ka	93.14	6.954	wt.%	0.433
S	Ka	951.81	59.888	wt.%	0.378
Ca	Ka	57.77	3.943	wt.%	0.352
Cu	Ka	13.30	1.952	wt.%	0.446
Zn	Ka	63.30	11.118	wt.%	0.519
Br	Ka	22.86	16.144	wt.%	1.360
			100.000	wt.%	Total

kV	20.0
Takeoff Angle	14.4°
Elapsed Livetime	100.0

Permeability: Air permeability was measured at two temperatures (21°C and 65°C). Method ASTM D1434-82, procedure V was used.[2-4, 23-26] The units on permeability are cc air at STP-cm/cm^2-sec atm. The apparatus by which permeability was measured works on the principles described by G. J. van Amerongen.[2] The gas cell is made of two parts of steel, containing gas chambers separated form each other by a rubber membrane (Figure 8). The gas was introduced into the lower chamber, which the upper chamber was connected to a volume gauge (Figure 9). The volume changes were recorded (Figure 10). The permeability was calculated using the equations in ASTM D1434.[4] The testing was performed with either a 66.4 cm^2 surface area permeability cell and a 8.04 cm^2 surface area permeability cell at 21°C.

Figure 8: Preparation for Permeability Test

Figure 9: Ready to Start Permeability Test

Figure 10: Permeability Test in Progress

Results and Discussion

Pyrolysis-gas chromatography/flame ionization detector (pyrolysis-GC/FID) Analysis of Tire Innerliners:

Forty three tire innerliners were analyzed by Pyrolysis-GC/FID. Seventeen model compounds were analyzed by Pyrolysis-GC/FID as standards for tire innerliner polymer identification. The peak identification is shown in Table 1 and Figures 11-13 for SBR (type1502), BIIR (ExxonMobil 2222), and NR (SMR-L), respectively. The peaks for isobutylene, isoprene, butadiene, and styrene were used for the calibration curves (Figures 14-17). Two tire innerliners were run twice (1030 and 1132) and showed good repeatability. The pyrolysis-gc/fid analysis was combined with XRF (bromine and chlorine determination) to qualitatively determine the butyl polymer types. The butyl type in six tires (2039, 2250, 2313, 2378, 2404, and 2551) was determined by EDAX.

Table 1: Pyrolysis-GC/FID Peak Identification

Chemical	Peak Location (min)
isobutylene	3.9-4.1
Isobutylene trimer (probably)	22.5
Isobutylene trimer (probably)	23.1
isoprene	8.9-9.1
Isoprene dimer	22.8
butadiene	4.3
Butadiene dimer	16.99
Styrene	19.95-20.0

Figure 11: Pyrolysis-GC/FID Analysis of SBR (1502) Gum Polymer

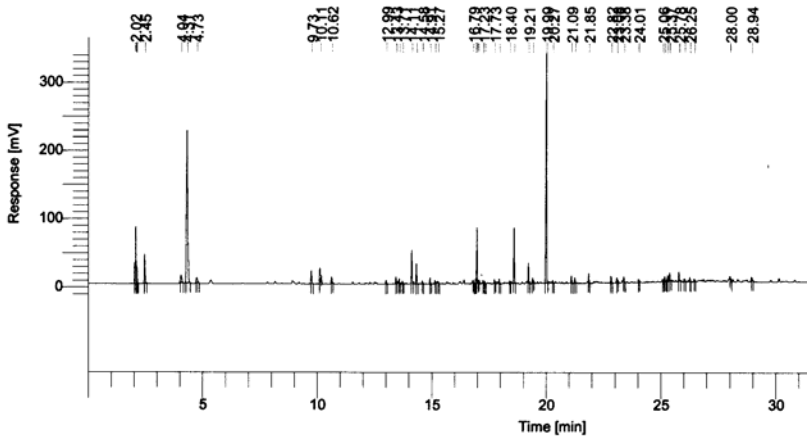

Figure 12: Pyrolysis-GC/FID Analysis of BIIR Gum Polymer

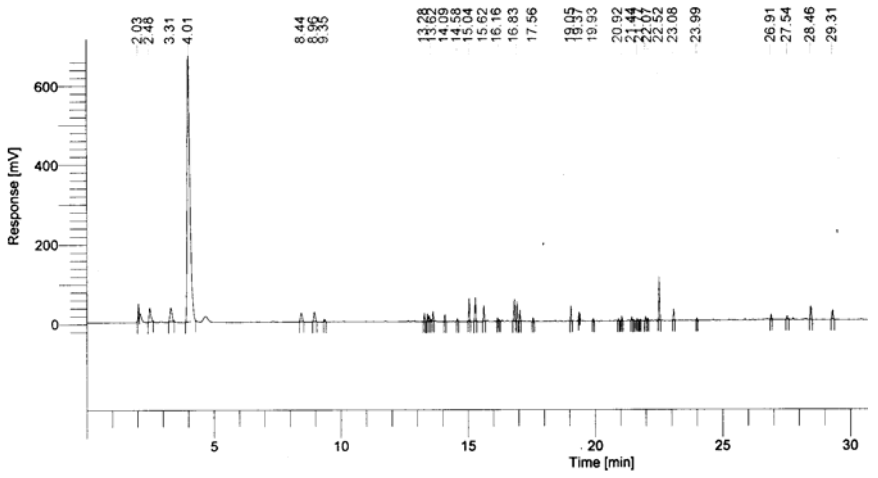

Figure 13: Pyrolysis-GC/FID Analysis of Natural Rubber Gum Polymer

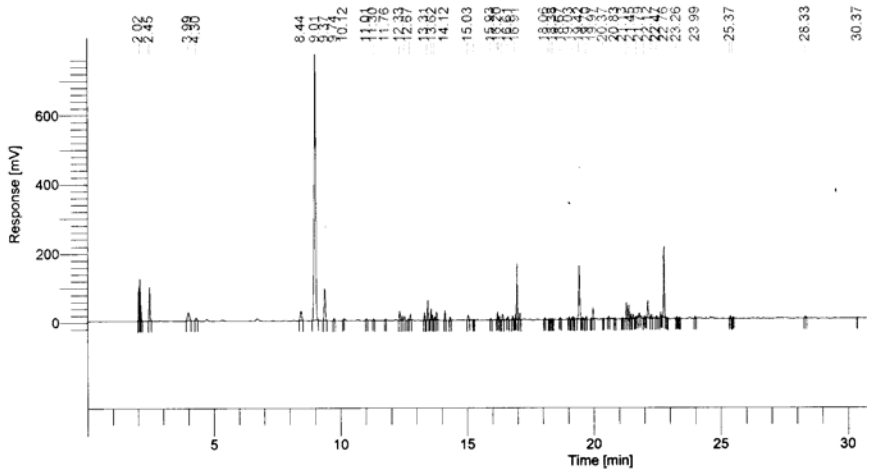

Figure 14: Pyrolysis-GC/FID Calibration Curve for Polyisobutylene based on Isobutylene

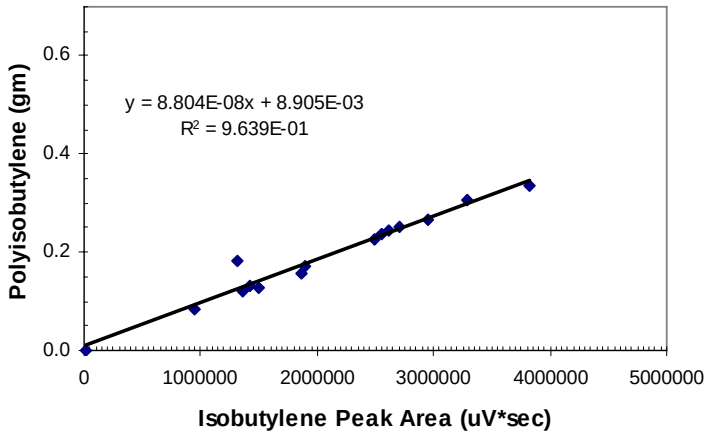

Figure 15: Pyrolysis-GC/FID Calibration Curve for Polyisoprene based on Isoprene

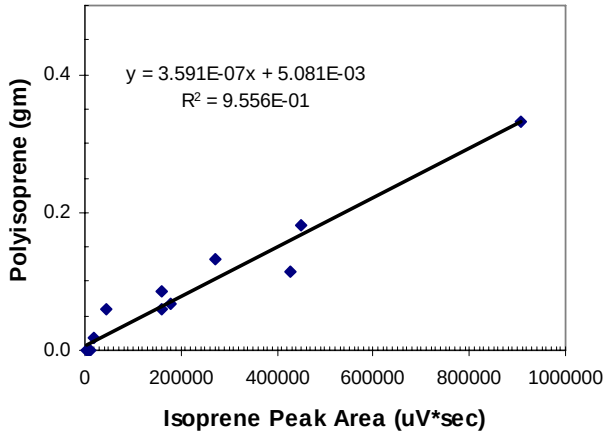

Figure 16: Pyrolysis-GC/FID Calibration Curve for Styrene Butadiene Polymer based on Styrene

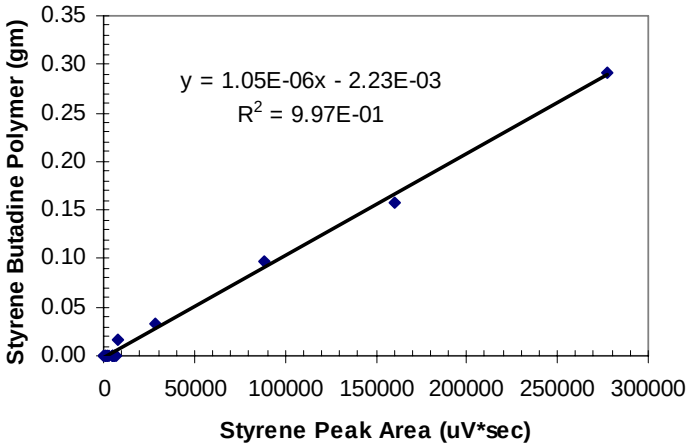

Figure 17: Pyrolysis-GC/FID Calibration Curve for Styrene Butadiene Polymer based on Butadiene

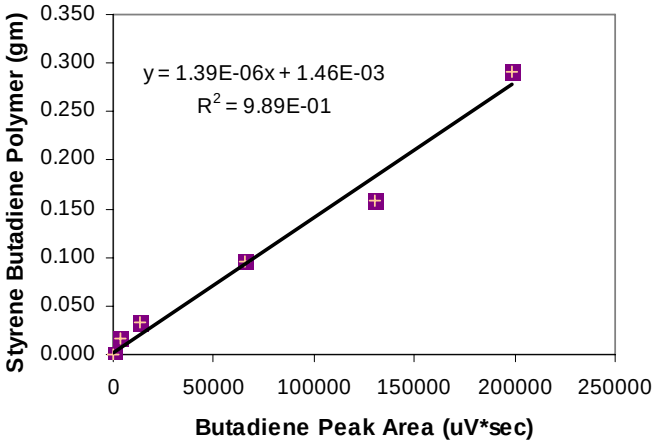

Pyrolysis-gas chromatography/mass spectroscopy (pyrolysis-GC/MS) Analysis of Tire Innerliners:

Twenty two tire innerliners were analyzed by Pyrolysis-GC/MS to confirm their compositional analysis. Seventeen model compounds were analyzed by Pyrolysis-GC/MS as standards for tire innerliner polymer identification. The peak identifications are shown in Table 2. The peaks for isobutylene, isobutylene tetramer, isoprene, isoprene dimer, styrene, and butadiene dimmer were used for the calibration curves (Figures 18-23). One tire innerliner was run twice (2126) and showed good repeatability.

Table 2: Pyrolysis-GC/MS Peak Identification

chemical	pyrolysis-gc/ms peak location

isobutylene	2.74-2.83
isobutylene tetramer	26.78-26.81
isoprene	7.33-7.60
isoprene dimer	20.84-20.88
styrene	18.13-18.15
butadiene dimer	16.79-16.84

Figure 18: Pyrolysis-GC/MS Calibration Curve for Polyisobutylene based on Isobutylene

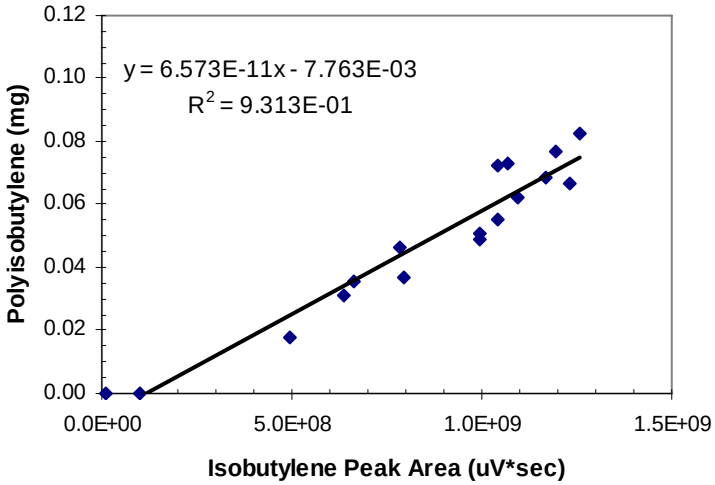

Figure 19: Pyrolysis-GC/MS Calibration Curve for Polyisobutylene based on Isobutylene Tetramer

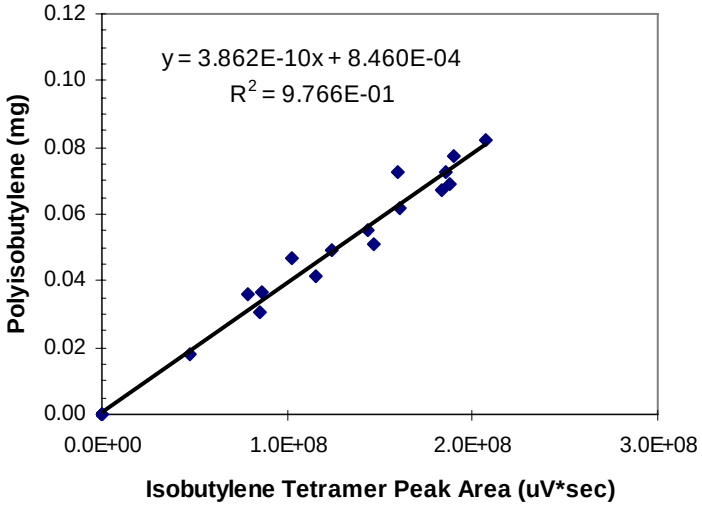

Figure 20: Pyrolysis-GC/FID Calibration Curve for Polyisoprene based on Isoprene

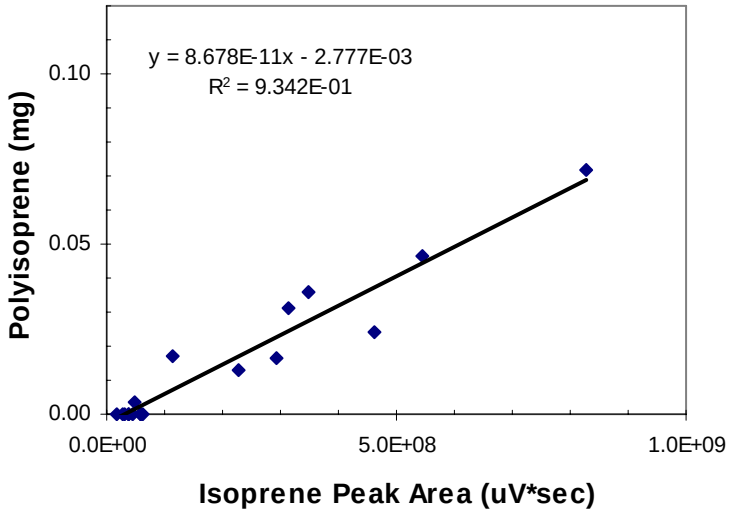

Figure 21: Pyrolysis-GC/FID Calibration Curve for Polyisoprene based on Isoprene Dimer

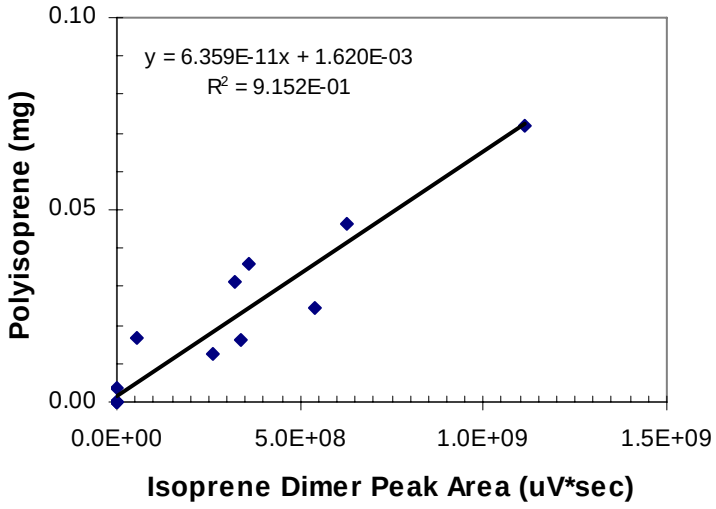

Figure 22: Pyrolysis-GC/FID Calibration Curve for Styrene Butadiene Polymer based on Styrene

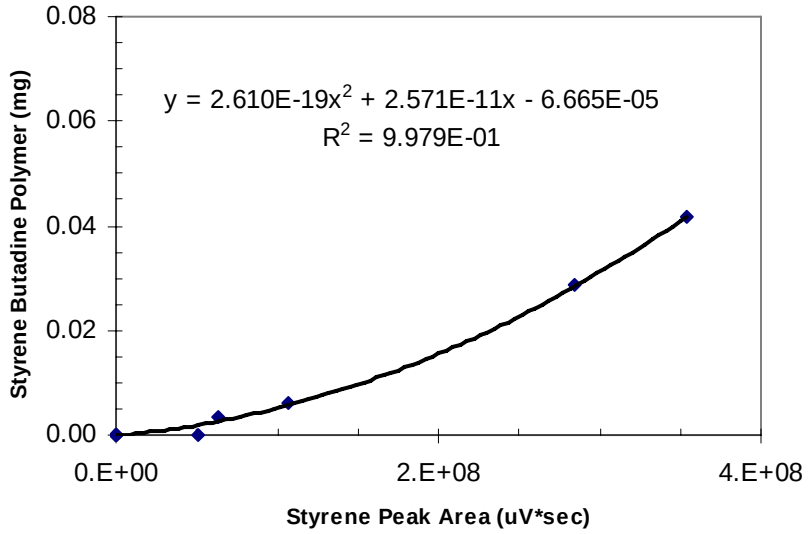

Figure 23: Pyrolysis-GC/FID Calibration Curve for Styrene Butadiene Polymer based on Butadiene Dimer

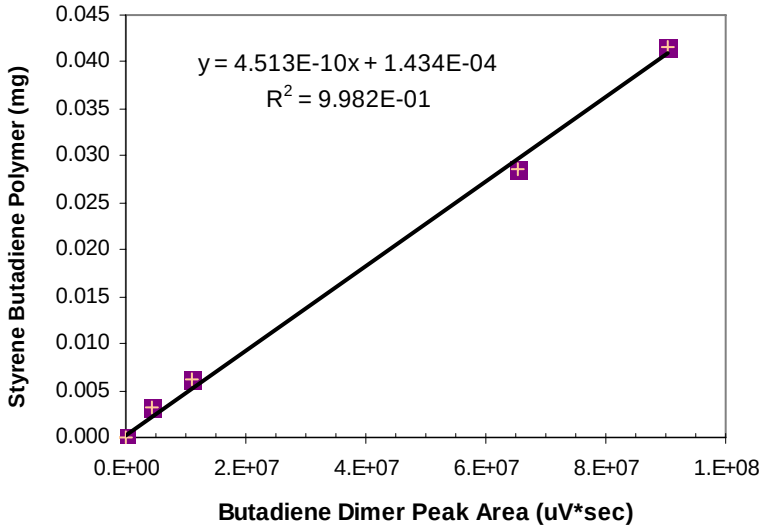

XRF Analysis of Tire Innerliners:

Thirty seven tire innerliners were analyzed by X-ray Fluorescence (XRF). The calibration curves from the model compounds were used to determine the butyl type (halogen type). Five model compounds were analyzed by X-ray Fluorescence (XRF) (Table 3). Calibration curves were determined from the model compound data (Figures 24-25). The results were grouped in categories: Major (>1%), Minor (<100 ppm to 1%), Trace (<100 ppm) by weight in the sample. The X-ray fluorescence data was combined with the pyrolysis-gc/fid and the pyrolysis-gc/ms data to determine the halogen type in

the butyl polymer. The halogen type in six of the thirty seven innerliners was determined by EDAX, which is discussed in the next section.

Table 3: XRF Analysis Results of Model Compounds

Model Compound Polymers	Bromine	Chlorine	Sulfur	Calcium	Iron	Potassium	Zinc
100 BIIR	Major		Major	Minor	Trace		Major
50/50 BIIR/NR	Major		Major	Minor	Trace	Minor	Major
100 CIIR		Minor	Major	Minor	Trace	Minor	Major
75/25 CIIR/NR		Minor	Major	Minor	Trace	Minor	Major
100 IIR			Major	Minor	Trace		Major
100 NR			Major	Trace	Trace	Minor	Major

*Grouped in categories: Major (>1%), Minor (<100 ppm to 1%), Trace (<100 ppm)

Figure 24: Correlation Between XRF Bromine Content and phr Bromobutyl

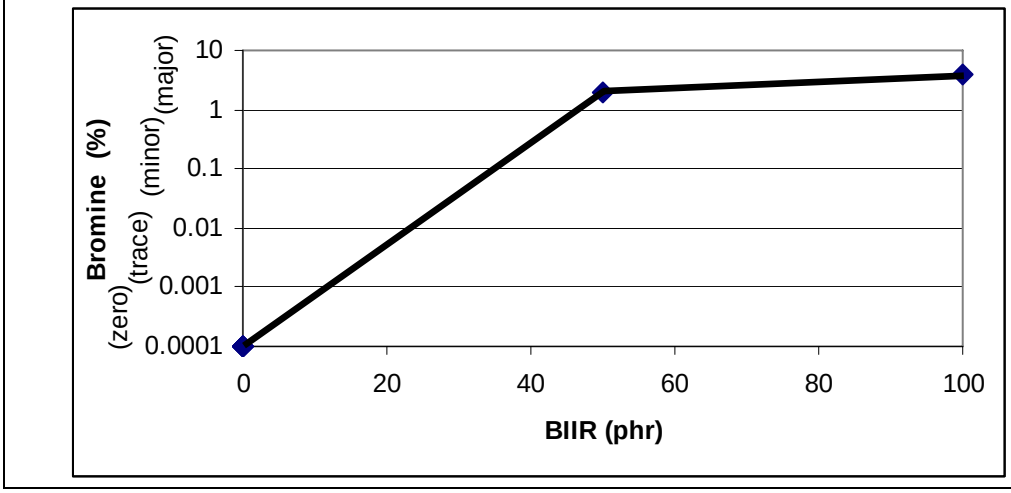

Figure 25: Correlation Between XRF Chlorine Content and phr Chlorbutyl

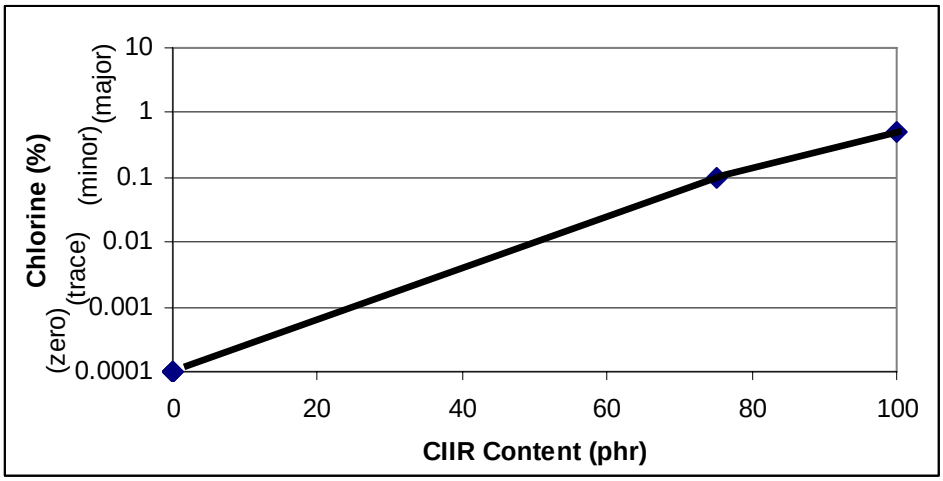

EDAX of Tire Innerliners (six additional tire innerliners):
Six tire innerliners were analyzed by EDAX (Tables 5-6). EDAX was used to determine the type of butyl polymer in the tire innerliner. The calibration curves from the model compounds were used to determine the butyl type (halogen type). Five model compounds were analyzed by EDAX (Table 4). The bromine intensity correlated with the phr of bromobutyl (Figure 26) and the chlorine intensity correlated with chlorobutyl loading (Figure 27). The EDAX data was combined with the pyrolysis-gc/fid and the pyrolysis-gc/ms data to determine the halogen type in the butyl polymer.

Table 4: EDAX of Model Compounds

	Polymers	100 BIIR	60/40 BIIR/NR	40/60 BIIR/NR	100CIIR	75/25 CIIR/NR
	Element	Intensity (c/s)	Intensity (c/s)	Intensity (c/s)	Intensity (c/s)	Intensity (c/s)
1	Silicon	37.6	58.3	63.5	32.0	20.6
2	Sulfur	455.3	525.4	1083.9	705.3	652.2
3	Chlorine				368.7	264.6
4	Potassium		17.5	11.0		
5	Calcium	62.1	40.0	26.8	28.2	19.5
6	Zinc	76.2	68.8	122.8	63.4	161.8
7	Bromine	31.4	17.6	13.8		

Figure 26: Correlation Between Bromine Intensity and phr Bromobutyl

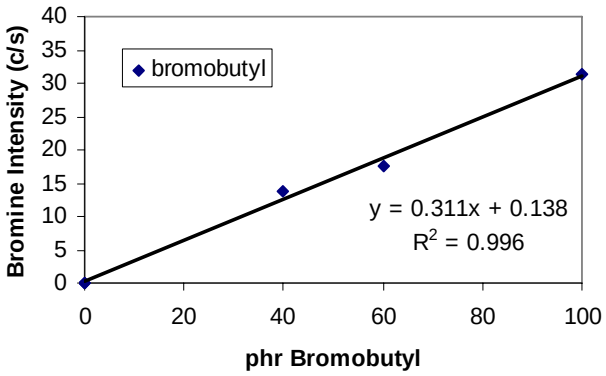

Figure 27: Correlation Between Chlorine Intensity and phr Chlorobutyl

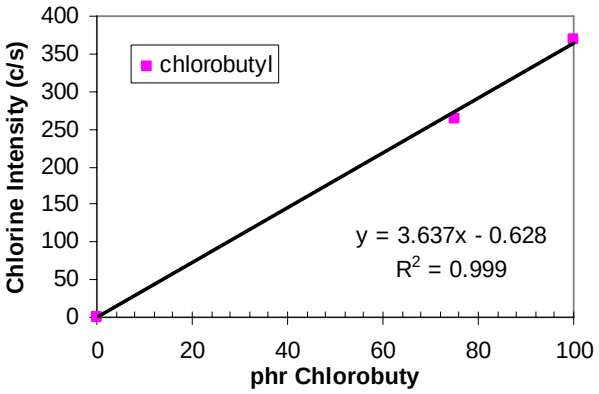

Table 5: EDAX Results (for Bromine and Chlorine)

Tire Number	2039	2250	2313	2378	2404	2551
Element	Intensity (c/s)	Intensity (c/s)	Intensity (c/s)	Intensity (c/s)	Intensity (c/s)	Intensity (c/s)
Chlorine	0.00	34.6	200	17.0	11.1	137
Bromine	24.5	23.3	0.00	3.40	2.84	3.83

Table 6: EDAX Prediction of Tire Innerliner Polymers

Tire Number	2039	2250	2313	2378	2404	2551
polymer	phr	phr	phr	phr	phr	phr
chlorobutyl	0	0	55	0	0	38
bromobutyl	78	74	0	0	0	0

Innerliner Composition Summary

The innerliner analysis is shown in Table 7. The pyrolysis-gc/fid and pyrolysis-gc/ms analysis was combined with XRF (bromine and chlorine determination) to qualitatively determine the butyl polymer types. The butyl type in six tires (2039, 2250, 2313, 2378, 2404, and 2551) was determined by EDAX.

Table 7: Compositional Analysis Summary					
NHTSA Tire #	Pyr-GC/FID+MS Composition (%)	Comment	Butyl Type based on XRF (or EDAX)	Manufacturer	Plant Code
2012	84/16-IIR/NR	Private Brand	IIR	Cooper	UT
2039	83/17-IIR/NR	Private Brand	BIIR	Cooper	UP
2040	83/17-IIR/NR	Private Brand	CIIR	Cooper	UT
2065	70/30-IIR/NR	Run-Flat	CIIR	Goodyear	EU
2113	93/7-IIR/NR		BIIR	Goodyear	PD
2126	92/8-IIR/NR		BIIR	Goodyear	PJ
2135	72/28-IIR/NR		BIIR	Pirelli	XL
2140	72/28-IIR/NR		BIIR	Yokahama	CC
2165	83/17-IIR/NR	Nokian Brand	CIIR	Cooper	UP
2178	48/37/15-IIR/NR/PBD		CIIR	Nokia	YL
2212	85/15-IIR/NR		BIIR	Bridgestone	EJ
2226	83/17-IIR/NR		BIIR	Bridgestone	7X
2250	85/15-IIR/NR		BIIR	Bridgestone	VX
2269	83/17-IIR/NR		BIIR	Bridgestone	EP
2270	81/17/2-IIR/NR/SBR		BIIR	Bridgestone	0B
2313	73/23/4-IIR/NR/PBD	Private Brand	CIIR	Cooper	U9
2326	82/18-IIR/NR	Private Brand	BIIR	Cooper	UP
2339	87/11/2-IIR/NR/SBR	Private Brand	BIIR	Goodyear	PJ
2352	85/8/7-IIR/NR/PBD	Private Brand	BIIR	Goodyear	PJ
2365	86/14-IIR/NR	Private Brand	CIIR	Cooper	UT
2378	65/35-NR/SBR	Private Brand	N/A	Goodyear	PJ
2391	89/11-IIR/NR	Private Brand	CIIR	Cooper	U9
2404	82/18-NR/SBR	Private Brand	N/A	Goodyear	PB
2417	83/17-IIR/NR	Private Brand	BIIR	Cooper	UP
2429	85/15-IIR/NR	Private Brand	BIIR	Cooper	3D

Table 7: Compositional Analysis Summary					
NHTSA Tire #	Pyr-GC/FID+MS Composition (%)	Comment	Butyl Type based on XRF (or EDAX)	Manufacturer	Plant Code
2438	90/8/2-IIR/NR/PBD		BIIR	Goodyear	PJ
2456	56/38/6-IIR/NR/SBR		BIIR	Continental	A3
2469	100 IIR	polystyrene resin	BIIR	Michelin	B7
2482	89/11-IIR/NR		BIIR	Michelin	ED
2495	61/30/9-IIR/NR/SBR		BIIR	Continental	AC
2501	81/19-IIR/NR		BIIR	Bridgestone	7X
2526	66/21/13-IIR/NR/SBR		BIIR	Continental	A3
2551	55/37/8-IIR/NR/SBR		CIIR	Continental	P5
2576	70/30-IIR/NR		BIIR	Hankook	T7
2601	100 IIR	polystyrene resin	BIIR	Michelin	B7
2626	43/47/11-IIR/NR/SBR		BIIR	Sumitomo	V4
2651	53/47-IIR/NR		BIIR	Toyo	9T
1030	100 IIR	polystyrene resin	BIIR	Michelin	AP
1030	100 IIR	polystyrene resin	BIIR	Michelin	AP
1132	100 IIR	polystyrene resin	BIIR	Michelin	B3
1132	100 IIR	polystyrene resin	BIIR	Michelin	B3
1227	84/7/9-IIR/NR/PBD	Private label	BIIR	Goodyear	PJ
1337	86/14-IIR/SBR		BIIR	Bridgestone	VN
1427	70/30-IIR/NR		BIIR	Continental	A3
1530	92/6/2-IIR/NR/PBD		BIIR	Goodyear	M6

The innerliner compositions of tires of the same brand were compared. Many samples showed small amounts of SBR and/or PBD rubber which could be spurious data, or could come from small amounts of these polymers which may be added as recycled rubber. The addition of small amounts of uncured tire compounds (work-away) is less common in modern radial tires. However, the use of finely ground tire compounds in innerliners is increasing in popularity. The average formulations were similar by either method of identification (Table 8). The Bridgestone tires were estimated as an 85/15 bromobutyl/natural rubber compound. The Continental tires were approximately a 65/35

bromobutyl/natural compound. The Cooper tires were approximately 85/15 halobutyl/natural formulations, with chlorobutyl or bromobutyl rubber, varying by plant. The Goodyear tires were approximately a 90/10 bromobutyl/natural rubber formulation. Finally, the Michelin tires were approximately 100 phr bromobutyl compound, containing a high styrene resin.

Table 8: Composition Summary by Manufacturer

Tire Brand	Number of Samples (GC/FID : GC/MS)	HIIR Content by FID	HIIR Content by MS	NR Content by FID	NR Content by MS	SBR / PBD Content by FID	SBR / PBD Content by MS
Bridgestone	7 : 6	83.4 ± 2.0	85.3 ± 12.8	14.3 ± 6.4	12.9 ± 6.7	2.3 ± 5.2 (SBR)	1.8 ± 3.6 (SBR)
Continental	5 : 1	61.6 ± 6.4	72	31.2 ± 6.8	23	7.2 ± 4.8 (SBR)	5 (PBD)
Cooper	10 : 3	83.1 ± 4.1	82.3 ± 4.5	16.5 ± 3.1	16.3 ± 4.7	0.4 ± 1.3 (PBD)	1.7 ± 1.5 (PBD)
Goodyear	7 : 7	89.0 ± 3.7	89.6 ± 2.8	7.9 ± 1.6	5.4 ± 1.9	1.3 ± 2.6 (SBR) 2.0 ± 2.2 (PBD)	2.0 ± 2.2 (SBR) 2.9 ± 3.7 (PBD)
Michelin	7 : 1	98.4 ± 4.2	100	1.6 ± 4.2	0	0	0

Permeability of Tire Innerliners:

Six model compounds (L21150-154-1-6) were analyzed for air permeability by ASTM method D1434-82 (Table 9) and were compared to literature values (Table 10).[2,3,10,11,27,28] The experimental results compared closely to literature data. The results were reported in units of cm^3STP-cm/cm^2-sec-atm, but a conversion table is supplied in Table 11. The testing was performed with a 66.4 cm^2 surface area permeability cell and a 8.04 cm^2 surface area permeability cell at 21°C (Figure 28). Twelve more (liners 1-11,19) model compounds were analyzed for permeability by ASTM method D1434-82. The results were reported in units of cm^3STP-cm/cm^2-sec-atm (Tables 12 and 13). The permeability values of the model compounds were compared to literature values and good agreement was observed. The testing was performed with 66.4 cm^2 surface area at 21°C and 65°C (Figures 29 and 30).

Table 9: Model Compound Permeability Data

Compound #	Temperature (degC)	BIIR	CIIR	IIR	NR	SBR	permeability (cm^3STP-cm/cm^2-sec-atm)	Cell Size (cm^2)
L21150-154-1	21	100					5.3E-09	66.4
L21150-154-2	21	80			20		9.2E-09	66.4
L21150-154-3	21	80				20	8.1E-09	66.4
L21150-154-4	21				100		5.0E-08	66.4
L21150-154-5	21		100				6.4E-09	66.4
L21150-154-6	21		80		20		9.8E-09	66.4

L21150-154-1	21	100					1.8E-08	8.04
L21150-154-2	21	80			20		1.5E-08	8.04
L21150-154-3	21	80				20	1.3E-08	8.04
L21150-154-3	21	80				20	1.8E-08	8.04
L21150-154-4	21				100		6.4E-08	8.04
L21150-154-5	21		100				2.3E-08	8.04
L21150-154-6	21		80		20		1.9E-08	8.04

Table 10: Permeability Literature Values

Polymer	Temperature (°C)	permeability (cm^3STP-cm/cm^2-sec-atm) at 21°C	Reference
BIIR	21	3.0E-09	5
BIIR	21	3.6 to 4.6E-9	8
BIIR	25	3.2E-09	9
BIIR	25	3.8E-09	7
BIIR	65	2.7E-08	9
BIIR	65	4.3 to 7.0E-8	44
BIIR	65	2.8E-08	7
NR	21	3.6E-08	5
NR	25	4.2E-08	9
NR	65	2.1E-07	9

Table 11: Conversion Table

Sample #	permeability (cm^3STP-cm/cm^2-sec-atm)	permeability (cm^3STP-cm/cm^2-sec-Pa)	permeability (cm^3STP-cm/cm^2-sec-cmHg)
L21150-154-1(example)	5.30E-09	5.23E-14	6.97E-11
Unit Conversion	1	9.86E-06	1.316E-02

Figure 28: Permeability of Model Compounds at 21°C as a Function of Butyl Content

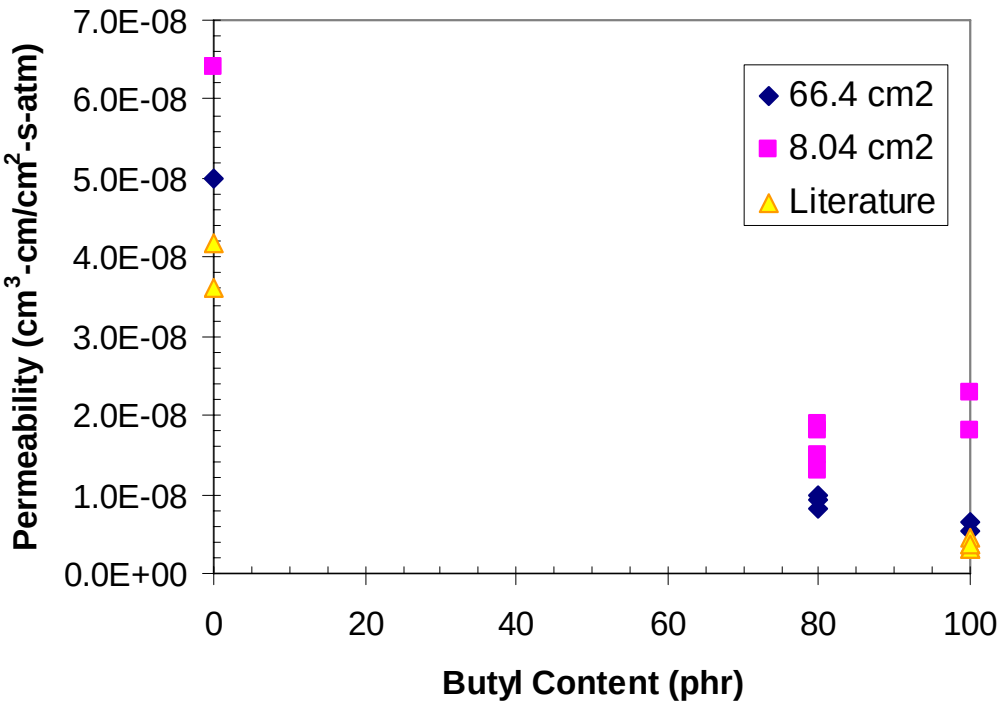

Table 12: 21°C Model Compound Permeability Data (66.4 cm^2 Cell Size)

Sample ID	Temperature (degC)	phr IIR	phr CIIR	phr BIIR	phr NR	Permeability (cm^3*cm/(cm^2*s*atm))
Liner #1	21			100		7.04E-09
Liner #2	21			80	20	7.00E-09
Liner #3	21			60	40	2.03E-08
Liner #4	21			50	50	5.53E-09
Liner #5	21			40	60	2.14E-08
Liner #6	21			20	80	4.61E-08
Liner #7	21		100			7.97E-09
Liner #8	21		80		20	8.67E-09
Liner #9	21		75		25	5.25E-09
Liner #10	21		60		40	1.02E-08
Liner #11	21	100				5.03E-09
Liner #19	21				100	5.32E-08

Table 13: 65°C Model Compound Permeability Data (66.4 cm^2 Cell Size)

Sample ID	Temperature (degC)	phr IIR	phr CIIR	phr BIIR	phr NR	Permeability (cm^3*cm/(cm^2*s*atm))
Liner #1	65			100		5.23E-08

Liner #2	65			80	20	6.66E-08
Liner #3	65			60	40	1.29E-07
Liner #4	65			50	50	2.22E-07
Liner #5	65			40	60	1.62E-07
Liner #6	65			20	80	2.99E-07
Liner #7	65		100			4.33E-08
Liner #8	65		80		20	7.86E-08
Liner #9	65		75		25	7.17E-08
Liner #10	65		60		40	7.03E-08
Liner #11	65	100				5.09E-08
Liner #19	65				100	4.06E-07

Figure 29: Permeability of Model Compounds at 21°C as a Function of Butyl Content

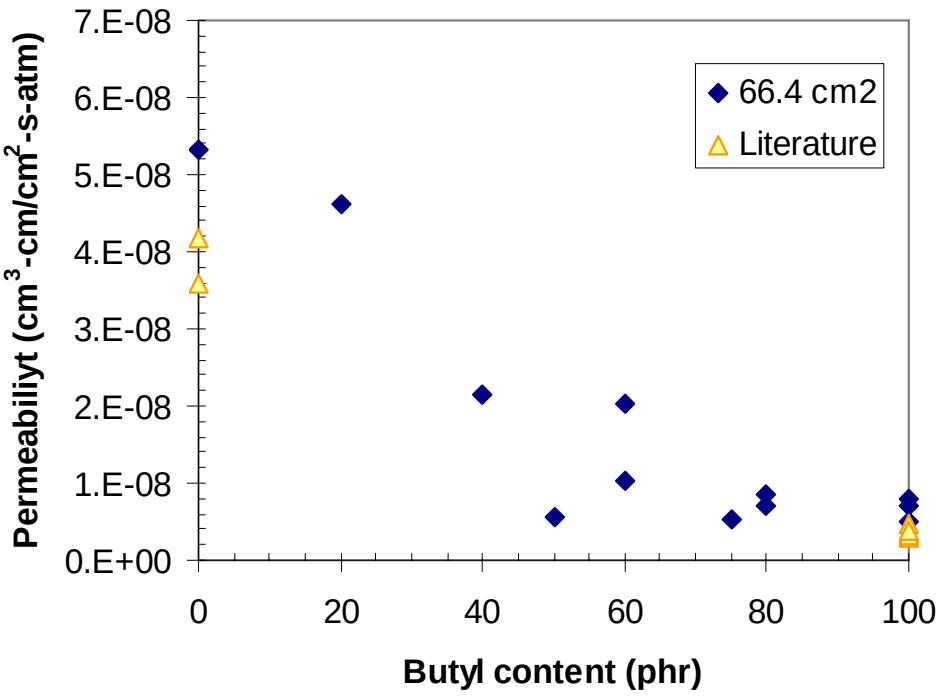

Figure 30: Permeability of Model Compounds at 65°C as a Function of Butyl Content

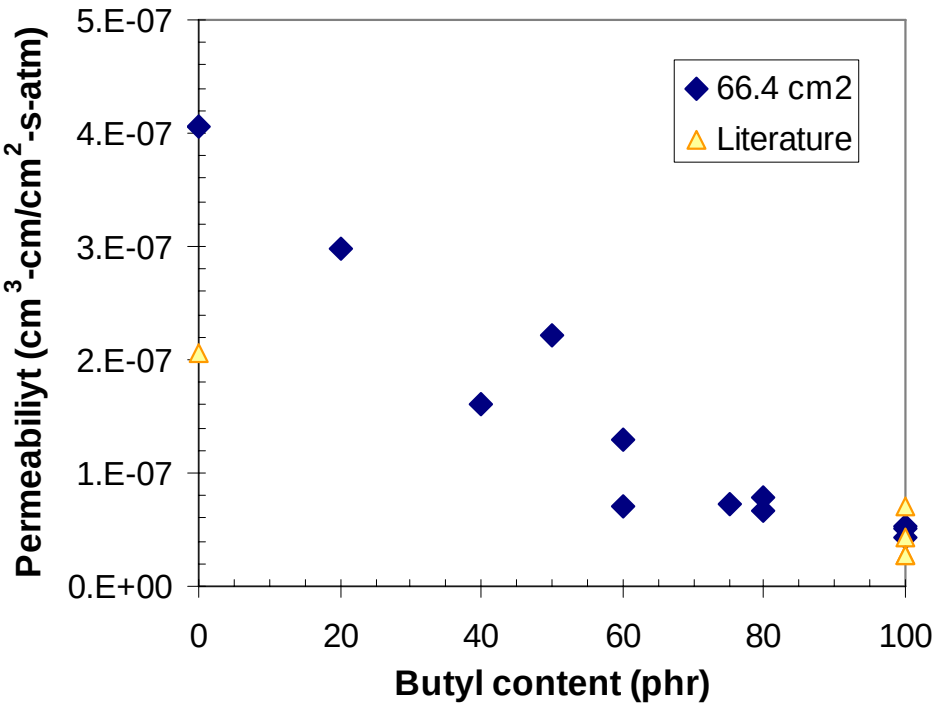

Forty three tire innerliners were analyzed for permeability by ASTM method D1434-82. The permeability values of extracted innerliners were compared to literature values.[2,3,10,11,27,28] The experimental results compared closely to literature values. The testing was performed with 8.04 cm^2 surface at 21°C and 65°C area because the of the size limitations associated with removing large flat slices of innerliner slices from tires. The results are shown in Figures 31-32 and Tables 14-15. Some data scatter may come from thickness non-uniformity. Some innerliners have a pattern imprint which could not be removed. The error bars are shown on the six innerliners which had repeat measurements. The confidence was about +/- 25%.

Table 14: Permeability Data at 21°C on Tire Innerliners

			Gas Permeability_(cm^2/(sec*atm))					
	pyr-gc/fid comp	phr butyl	First	Second	Third	Average	Std Dev	Confidence
2012	84/16-IIR/NR	84	1.07E-08			1.07E-08		
2039	83/17-IIR/NR	83	1.50E-08			1.50E-08		
2040	83/17-IIR/NR	83	1.66E-08			1.66E-08		
2065	70/30-IIR/NR	70	2.76E-08			2.76E-08		
2113	93/7-IIR/NR	93	1.96E-08			1.96E-08		

Table 14: Permeability Data at 21°C on Tire Innerliners								
			Gas Permeability_(cm^2/(sec*atm))					
	pyr-gc/fid comp	phr butyl	First	Second	Third	Average	Std Dev	Confidence
2126	92/8-IIR/NR	92	1.45E-08			1.45E-08		
2135	72/28-IIR/NR	72	1.65E-08			1.65E-08		
2140	72/28-IIR/NR	72	1.28E-08			1.28E-08		
2165	83/17-IIR/NR	83	2.82E-08			2.82E-08		
2178	48/37/15-IIR/NR/PBD	47	2.64E-08	1.99E-08		2.32E-08		
2212	85/15-IIR/NR	85	2.20E-08			2.20E-08		
2226	83/17-IIR/NR	83	1.18E-08			1.18E-08		
2250	85/15-IIR/NR	85	2.02E-08			2.02E-08		
2269	83/17-IIR/NR	83	2.24E-08			2.24E-08		
2270	81/17/2-IIR/NR/SBR	81	1.11E-08			1.11E-08		
2313	72/23/5-IIR/NR/PBD	72	2.52E-08			2.52E-08		
2326	82/18-IIR/NR	82	1.36E-08			1.36E-08		
2339	87/11/2-IIR/NR/SBR	87	7.93E-09			7.93E-09		
2352	85/8/7-IIR/NR/PBD	83	5.55E-09			5.55E-09		
2365	86/14-IIR/NR	86	2.03E-08			2.03E-08		
2378	65/35-NR/SBR	0	2.52E-08	8.39E-08		5.46E-08		
2391	89/11-IIR/NR	89	1.65E-08			1.65E-08		
2404	82/18-NR/SBR	0	7.05E-08			7.05E-08		
2417	83/17-IIR/NR	83	1.18E-08			1.18E-08		
2429	85/15-IIR/NR	85	2.47E-08			2.47E-08		
2438	90/8/2-IIR/NR/PBD	92	1.65E-08			1.65E-08		
2456	56/38/6-IIR/NR/SBR	56	1.38E-08			1.38E-08		
2469	100 IIR	100	1.29E-08			1.29E-08		
2469	100 IIR	100	1.78E-08			1.78E-08		
2482	89/11-IIR/NR	89	1.28E-08			1.28E-08		
2495	61/30/9-IIR/NR/SBR	61	2.28E-08			2.28E-08		

Table 14: Permeability Data at 21°C on Tire Innerliners								
			Gas Permeability_(cm^2/(sec*atm))					
	pyr-gc/fid comp	phr butyl	First	Second	Third	Average	Std Dev	Confidence
2501	81/19/- IIR/NR	81	1.30E-08			1.30E-08		
2526	66/21/13- IIR/NR/SBR	66	1.79E-08			1.79E-08		
2576	70/30- IIR/NR	70	1.87E-08			1.87E-08		
2601	100 IIR	100	2.06E-08			2.06E-08		
2626	43/47/11- IIR/NR/SBR	43	2.04E-08	9.75E-09		1.51E-08		
2651	53/47- IIR/NR	53	1.86E-08			1.86E-08		
1030	100 IIR	100	1.64E-08			1.05E-08	3.14E-09	2.41E-09
1025	100 IIR	100	1.19E-08	1.33E-08				
1026	100 IIR	100	8.03E-09					
1027	100 IIR	100	7.76E-09	8.37E-09	9.13E-09			
1028	100 IIR	100	7.35E-09	1.26E-08				
1132	100 IIR	100	1.72E-08			1.00E-08	5.35E-09	4.48E-09
1125	100 IIR	100	1.47E-08	6.67E-09				
1126	100 IIR	100	1.71E-08	5.56E-09				
1127	100 IIR	100	7.93E-09					
1128	100 IIR	100	6.23E-09	4.81E-09				
1227	84/7/9- IIR/NR/PBD	82	1.60E-08			1.04E-08	4.86E-09	4.06E-09
1225	84/7/9- IIR/NR/PBD	82	1.39E-08					
1226	84/7/9- IIR/NR/PBD	82	7.05E-09	7.60E-09				
1227	84/7/9- IIR/NR/PBD	82	1.82E-08	8.29E-09	5.06E-09			
1228	84/7/9- IIR/NR/PBD	82	7.36E-09					
1337	86/14- IIR/SBR	86	2.58E-08			1.79E-08	1.13E-08	8.70E-09
1306	86/14- IIR/SBR	86	1.98E-08	5.73E-09				
1308	86/14- IIR/SBR	86	1.90E-08	1.22E-08				
1319	86/14- IIR/SBR	86	4.27E-08	9.06E-09				
1333	86/14- IIR/SBR	86	1.82E-08	8.84E-09				
1427	70/30- IIR/NR	70	2.46E-08			1.82E-08	5.44E-09	4.19E-09
1425	70/30- IIR/NR	70	2.74E-08	1.73E-08				
1426	70/30- IIR/NR	70	2.02E-08	1.41E-08	1.08E-08			

Table 14: Permeability Data at 21°C on Tire Innerliners								
			Gas Permeability_(cm^2/(sec*atm))					
	pyr-gc/fid comp	phr butyl	First	Second	Third	Average	Std Dev	Confidence
1427	70/30-IIR/NR	70	1.70E-08	1.25E-08				
1428	70/30-IIR/NR	70	1.95E-08					
1530	92/6/2-IIR/NR/PBD	92	1.10E-08					
1525	92/6/2-IIR/NR/PBD	92	1.40E-08	9.83E-09				
1526	92/6/2-IIR/NR/PBD	92	1.46E-08					
1527	92/6/2-IIR/NR/PBD	92	1.55E-08	1.27E-08	9.50E-09	1.06E-08	4.41E-09	3.16E-09
1528	92/6/2-IIR/NR/PBD	92	1.29E-08	4.48E-09				
1530	92/6/2-IIR/NR/PBD	92	1.96E-09					

Figure 31: Permeability of Tire Innerliners at 21°C as a Function of Butyl Content

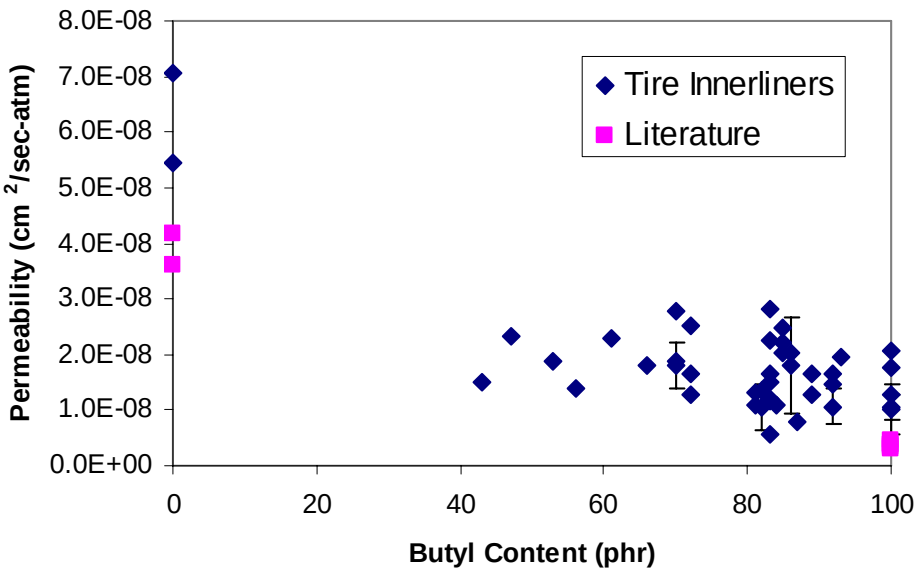

Table 15: Permeability Data at 65°C on Tire Innerliners								
			Gas Permeability_(cm^2/(sec*atm))					
	pyr-gc/fid comp	phr butyl	First	Second	Third	Average	Std Dev	Confidence
2012	84/16-IIR/NR	84	1.50E-07			1.5E-07		

Table 15: Permeability Data at 65°C on Tire Innerliners								
			Gas Permeability_(cm^2/(sec*atm))					
	pyr-gc/fid comp	phr butyl	First	Second	Third	Average	Std Dev	Confidence
2039	83/17-IIR/NR	83	1.66E-07			1.66E-07		
2040	83/17-IIR/NR	83	1.20E-07			1.20E-07		
2065	70/30-IIR/NR	70	6.83E-08			6.83E-08		
2113	93/7-IIR/NR	93	1.57E-07			1.57E-07		
2140	72/28-IIR/NR	72	1.22E-07			1.22E-07		
2178	48/37/15-IIR/NR/PBD	47	1.35E-07	5.58E-08		9.53E-08		
2212	85/15-IIR/NR	85	1.45E-07			1.45E-07		
2226	83/17-IIR/NR	83	8.88E-08			8.88E-08		
2269	83/17-IIR/NR	83	1.80E-07			1.80E-07		
2270	81/17/2-IIR/NR/SBR	81	5.26E-08			5.26E-08		
2326	82/18-IIR/NR	82	1.19E-07			1.19E-07		
2339	87/11/2-IIR/NR/SBR	87	1.62E-07			1.62E-07		
2352	85/8/7-IIR/NR/PBD	83	1.36E-07			1.36E-07		
2365	86/14-IIR/NR	86	3.79E-08			3.79E-08		
2378	65/35-NR/SBR	0	5.16E-07	5.05E-07		5.11E-07		
2391	89/11-IIR/NR	89	7.31E-08			7.31E-08		
2404	82/18-NR/SBR	0	4.86E-07			4.86E-07		
2417	83/17-IIR/NR	83	1.56E-07			1.56E-07		
2429	85/15-IIR/NR	85	5.21E-08			5.21E-08		
2456	56/38/6-IIR/NR/SBR	56	1.61E-07			1.61E-07		
2469	100 IIR	100	1.02E-07			1.02E-07		
2482	89/11-IIR/NR	89	8.56E-08			8.56E-08		
2495	61/30/9-IIR/NR/SBR	61	7.52E-08	6.90E-08		7.21E-08		
2501	81/19/-IIR/NR	81	1.36E-07			1.36E-07		
2526	66/21/13-IIR/NR/SBR	66	5.18E-08			5.18E-08		

Table 15: Permeability Data at 65°C on Tire Innerliners								
			Gas Permeability_(cm^2/(sec*atm))					
	pyr-gc/fid comp	phr butyl	First	Second	Third	Average	Std Dev	Confidence
2576	70/30-IIR/NR	70	2.11E-07			2.11E-07		
2601	100 IIR	100	7.58E-08			7.58E-08		
2626	43/47/11-IIR/NR/SBR	43	1.86E-07			1.86E-07		
2651	53/47-IIR/NR	53	1.51E-07			1.51E-07		
1030	100 IIR	100	6.26E-08	6.79E-08		6.94E-08	1.79E-08	1.38E-08
1029	100 IIR	100	9.49E-08	7.96E-08				
1031	100 IIR	100	3.81E-08	6.46E-08				
1032	100 IIR	100	9.42E-08	5.79E-08				
1028	100 IIR	100	6.51E-08					
1132	100 IIR	100	5.11E-08	6.62E-08		6.57E-08	2.66E-08	2.23E-08
1129	100 IIR	100	6.35E-08	4.59E-08				
1130	100 IIR	100	1.18E-07	5.23E-08				
1131	100 IIR	100	9.11E-08	3.74E-08				
1229	82/6/12-IIR/NR/PBD	82	7.01E-08	4.28E-08		5.92E-08	1.57E-08	1.32E-08
1230	84/7/9-IIR/NR/PBD	82	4.38E-08	7.22E-08				
1231	84/7/9-IIR/NR/PBD	82	3.90E-08					
1232	84/7/9-IIR/NR/PBD	82	8.17E-08	5.97E-08				
1226	84/7/9-IIR/NR/PBD	82	6.43E-08					
1337	86/14-IIR/SBR	86	5.78E-08			6.51E-08	2.04E-08	1.70E-08
1357	86/14-IIR/SBR	86	1.07E-07	6.68E-08				
1359	86/14-IIR/SBR	86	5.53E-08					
1368	86/14-IIR/SBR	86	3.57E-08	5.68E-08				
1308	86/14-IIR/SBR	86	7.07E-08	7.03E-08				
1429	70/30-IIR/NR	70	6.29E-08	8.18E-08		9.70E-08	2.78E-08	2.14E-08
1430	70/30-IIR/NR	70	6.03E-08	1.11E-07				

Table 15: Permeability Data at 65°C on Tire Innerliners								
			Gas Permeability_(cm^2/(sec*atm))					
	pyr-gc/fid comp	phr butyl	First	Second	Third	Average	Std Dev	Confidence
1431	70/30-IIR/NR	70	1.29E-07	1.04E-07				
1432	70/30-IIR/NR	70	9.71E-08	8.48E-08				
1426	70/30-IIR/NR	70	1.42E-07					
1530	92/6/2-IIR/NR/PBD	92	4.76E-08	7.95E-08		7.74E-08	2.09E-08	1.40E-08
1529	92/6/2-IIR/NR/PBD	92	7.27E-08	1.13E-07				
1531	92/6/2-IIR/NR/PBD	92	4.96E-08	8.08E-08				
1532	92/6/2-IIR/NR/PBD	92	6.71E-08	8.90E-08	6.92E-08			
1527	92/6/2-IIR/NR/PBD	92	1.10E-07					
1528	92/6/2-IIR/NR/PBD	92		7.34E-08				

Figure 32: Permeability of Tire Innerliners at 65°C as a Function of Butyl Content

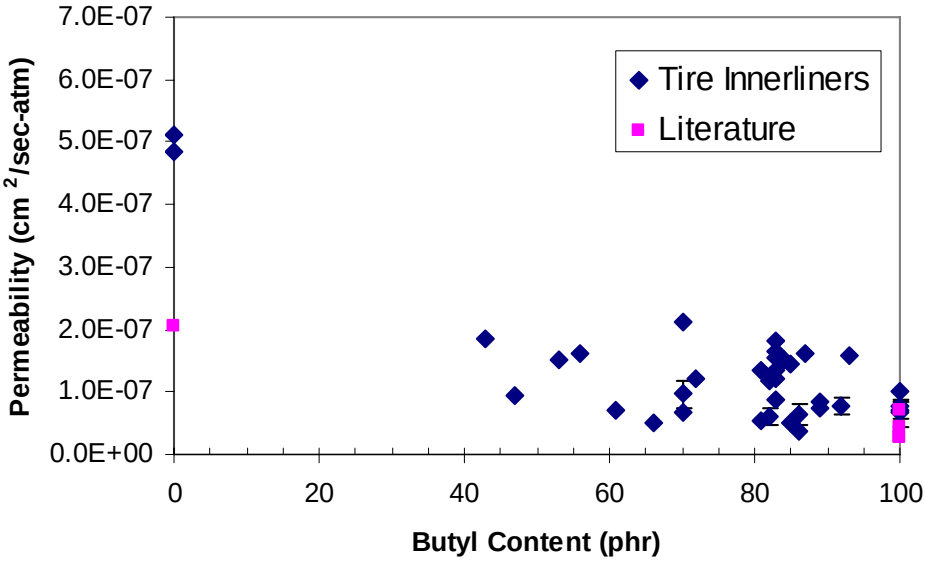

Summary and Conclusions:

The technique to extract slices of innerliner compound was developed. The techniques to quantify the polymers in innerliner compounds were developed using model compounds to establish a calibration curves. Calibration curves were established for key monomer

and fragment peaks in pyrolysis-gc/fid and pyrolysis-gc/ms. Calibration curves for XRF and EDAX were based on bromine and chlorine element peak intensity.

The innerliner compositions of forty-three tire types were determined. The compositions were determined by pyrolyisis-gc/fid and pyrolysis-gc/ms. The type of butyl was determined by either XRF or EDAX. The permeabilities of these tire innerliners were found to agree with literature data and to be a function primarily of polymer composition.

References:

1. The Phoenix Tire DATAset Version 4.0 at public website http://www-nrd.nhtsa.dot.gov/vrtc/ca/tires.htm
2. G J van Amerongen, *Journal of Applied Physics* **17**, 972 (1946).
3. G J van Amerongen, *Rubber Chemistry and Technology* , **37**, 1065 (1964).
4. ASTM Method D1434
5. B Costemalle, *Tire Science ad Technology* **20(4)**, 200 (1992).
6. D. M. Coddington, *Rubber Chemistry and Technology* **52(5)** (1979).
7. S. Dalpe and N. J. Pukas, ExxonMobil Technical Literature, **No 92PLYM 173** (1992).
8. J E Tombs, Presentation at a meeting of the Rubber Division, ACS, Paper No 40 (1994).
9. S. Dalpe and N. J. Pukas, ExxonMobil Technical Literature, **No 91PLYM 91** (1991).
10. N. L. Bakowski, E. C. Bender, and T. O. Munson, *Journal of Analytical And Applied Pyrolysis* **8** 483 (1985).
11. E. J. Levy and T. P. Wampler, *Journal of Chemical education* **63(3)** A64 (1986).
12. T. P. Wampler, G. A. Bishea, and W. J. Simonsick, *Journal of Analytical and Applied Pyrolysis* **40-41** 79 (1997).
13. M. J. Matheson, T. P. Wampler, L Johnson, L Atherly, L Smucker, *American Laboratory* May 24C (1997).
14. T. P. Wampler, *LC-GC Current Trends and Developments in Sample Preparation* **17(95)** S14 (1999).
15. T. P. Wampler, *Journal of Chromatography A* **842** 207 (1999).
16. T. P. Wampler, *Journal of Analytical Applied Pyrolysis* **72** 1 (2004).
17. M. Phair and T. P. Wampler, *Rubber World* **215** 30 (1997).
18. M. J. Matheson, T. P. Wampler, and W. J. Simonsick, *Journal of Analytical Applied Pyrolysis* **29** 129 (1994).
19. T. Wampler, *LabPlus International* September 6 (2004).
20. T. Wampler, "Polymer Degradation Mechanisms Encountered in Pyrolysis-GC/MS" Field Application Report, www.perkinelmer.com.
21. B. M. Trzcinska, *Chemia Analityczna* **51(1)** 147 (2006).
22. D. C. M. Squirrell, "Analysis plastic materials: X-ray fluorescence examination of volatile liquids with the Philips PW 1540 spectrometer," in *Proc SAC Conference*, 102 (1965).
23. G. J. Van Amerongen, *Rubber Chemistry and Technology* **28** 821 (1955).
24. G. J. Van Amerongen, *Rubber Chemistry and Technology* **24** 109 (1951).
25. G. J. Van Amerongen, *Rubber Chemistry and Technology* **20** 479 (1947).

26. K. Haraya and S-T Hwang, *Journal of Membrane Science* **71** 13 (1992).
27. J Brandrup, E H Immergut, E A Grulke, editors, “Polymer Handbook,” Fourth Edition, John Wiley & Sons, New York, 1999.
28. K T Gillen M Celina, Micheal Keenan, *Rubber Chemistry and Technology* **73 No 2** 265 (2000).
29. H. Kaidou and A. Ahagon, RUBBER CHEM. TECHNOL. 63, 698 (1990).
30. J M Baldwin and D R Bauer, *Rubber Chem. and Tech.* **81**, 338 (2008).
31. A. Pannikottu and E. R. Terrill, Test Report to National Highway Transportation Agency, “Study on Crosslink Network in Tire Beltcoat Compounds”, April 17, 2006.